Vol 12 No 7, July 2003
1009-1963/2003/12(07)/0803-06

Chinese Physics

© 2003 Chin. Phys. Soc.
and IOP Publishing Ltd

The penetration, diffusion and energy deposition of high-energy photon*

Luo Zheng-Ming(罗正明)[a], Gou Cheng-Jun(勾成俊)[a], and Wolfram Laub[b]

[a] *Institute of Nuclear Science and Technology, Sichuan University and Key Laboratory for Radiation Physics and Technology of the Education Ministry of China, Chengdu* 610064, *China*

[b] *Radiation Oncology, William Beaumont Hospital,* 3601 *West 13 Mile Road, Royal Oak, Michigan* 48073-6769, *USA*

(Received 26 December 2002; revised manuscript received 18 March 2003)

This paper presents a new theory for calculating the transport of high-energy photons and their secondary charged particles. We call this new algorithm characteristic line method, which is completely analytic. Using this new method we cannot only accurately calculate the transport behaviour of energetic photons, but also precisely describes the transport behaviour and energy deposition of secondary electrons, photoelectrons, Compton recoil electrons and positron–electron pairs. Its calculation efficiency is much higher than that of the Monte Carlo method. The theory can be directly applied to layered media situation and obtain a pencil-beam-modelled solution. Therefore, it may be applied to clinical applications for radiation therapy.

Keywords: high-energy photon, energy deposition, characteristic line method
PACC: 8250J, 3280, 0200

1. Introduction

Of late years the investigation on photon transport becomes a hot point in medical physics community.[1] Historically, photon transport investigation started from the period of the discovery of x-rays. During that period some classical theories and algorithms for photon diffusion in planet atmosphere were developed.[2–4] Later, the need for nuclear power and nuclear technology largely promoted the investigation on photon transport theory and algorithms. The moment method and Monte Carlo simulation were developed during this period.[5–9] Especially, the Monte Carlo method was greatly developed during this period.[10,11] Since the publication of the ICRU Report 24 in 1976, international medical physics community has understood that the rigorous dose control in radiation therapy is necessary. According to ICRU Report 24, the total dose error for radiation therapy should be limited to within 5%, which means the error of photon dose calculation should be within 2–3%. This is a very rigorous requirement, because no theory or algorithm can meet the difficult requirement in the 1970s. Since ICRU Report 24 was published, it cannot be said that the task has been completely solved now; however, great progress has still been made. Among these developments the progress of Monte Carlo method is notable due to the extremely enhancing of computer performance. In spite of this, much progress has still been made. The C/S method based on Monte Carlo calculation has made a breakthrough in clinical applications of radio-therapeutic technology.[11–15] Recently, Siantar *et al*[16] by using a parallel computer with 16 CPUs, have made the Monte Carlo method directly applicable to clinical radiotherapy.

This paper includes five sections: the second section describes photon theories; the third section deals with theories on secondary electron transport and energy deposition, and algorithms as well; a good number of calculation results are given in the fourth section, which show the validity and precision of our present theory; a brief summary is presented in the last section.

2. The transport of high-energy photons in homogeneous slab media

2.1. The transport equation for photons

*Project supported by the National Natural Science Foundation of China (Grant No 10075033) and the International Atomic Energy Agency (Grant No 8064/RB).

Under the condition of one-dimensional slab geometry the transport equation for photons reads

$$\mu\frac{\partial N}{\partial x} = -\Sigma(E)N(x,\mu,E) + \int_{4\pi}\mathrm{d}\boldsymbol{u}'\int_{E}^{E_0}\mathrm{d}E'N(x,\mu',E')K(E',E;\boldsymbol{u}\cdot\boldsymbol{u}') + \delta(x)\delta(E-E_0)\delta(1-\mu)/2\pi, \quad (1)$$

where $N(x,\mu,E)$ is the distribution function of photons, also called differential fluence of photons, $N(x,\mu,E)\mathrm{d}s\mathrm{d}\boldsymbol{u}\mathrm{d}E$ represents the number of photons at the depth of x with energy between E and $E+\mathrm{d}E$, and directions between $\boldsymbol{u}$ and $\boldsymbol{u}+\mathrm{d}\boldsymbol{u}$ passing through a small area $\mathrm{d}s$ perpendicular to $\boldsymbol{u}$ direction, and $\Sigma(E)$ is the mass attenuation coefficient of photons with energy E, which is given by

$$\Sigma(E) = \frac{N_A}{A}(\sigma_{\mathrm{PE}} + Z\sigma_{\mathrm{c}} + \sigma_{\mathrm{pair}}), \quad (2)$$

where N_A is Avogadro constant, A is the atomic weight of the medium, Z is the atomic number, σ_{PE} is the total cross section of photoelectric effect, σ_{pair} is the total cross section of electron pairs. $k(E,E';\boldsymbol{u}\cdot\boldsymbol{u}')\mathrm{d}E'\mathrm{d}\boldsymbol{u}'$ denotes the transition probability of a photon passing through a medium with a unit mass thickness, its energy varying from E to $E'\to E'+\mathrm{d}E'$ and directions varying from $\boldsymbol{u}$ to $\boldsymbol{u}\to\boldsymbol{u}'+\mathrm{d}\boldsymbol{u}'$; obviously,

$$k(E,E';\boldsymbol{u}\cdot\boldsymbol{u}') = \frac{N_A Z}{A}\sigma_{\mathrm{c}}(E,E')\delta\left(\frac{mc^2}{E'} - \frac{mc^2}{E} - 1 + \boldsymbol{u}\cdot\boldsymbol{u}'\right)/2\pi. \quad (3)$$

Eq. (1) is the photon transport equation. The photon beam can be decomposed into uncollided photon beam $N^{(0)}$, single scattered photon beam $N^{(1)}$ and multiple scattered photon beam $N^{(m)}$. So we have

$$N = N^{(0)} + N^{(1)} + N^{(m)}. \quad (4)$$

Substituting Eq.(4) into Eq.(1), we obtain equations which $N^{(0)}$, $N^{(1)}$ and $N^{(m)}$ satisfy. They are, respectively,

$$\mu\frac{\partial N^{(0)}}{\partial x} = -\Sigma(E)N^{(0)} + \delta(x)\delta(E-E_0)\delta(1-\mu)/2\pi, \quad (5)$$

$$\mu\frac{\partial N^{(1)}}{\partial x} = -\Sigma(E)N^{(1)} + \int_{4\pi}\mathrm{d}\boldsymbol{u}'\int_{E}^{E_0}\mathrm{d}E'N^{(0)}(x,\mu,E')K(E',E;\boldsymbol{u}\cdot\boldsymbol{u}'), \quad (6)$$

$$\mu\frac{\partial N^{(m)}}{\partial x} = -\Sigma(E)N^{(m)} + \int_{4\pi}\mathrm{d}\boldsymbol{u}'\int_{E}^{E_0}\mathrm{d}E'N^{(m)}(x,\mu',E')K(E',E;\boldsymbol{u}\cdot\boldsymbol{u}') + \int_{4\pi}\mathrm{d}\boldsymbol{u}'\int_{E}^{E_0}\mathrm{d}E'N^{(1)}(x,\mu',E')K(E',E;\boldsymbol{u}\cdot\boldsymbol{u}'). \quad (7)$$

2.2. Un-collided photons' differential fluence

The un-collided photons' differential fluence is determined by Eq.(5). The solution to Eq.(5) is very simple. That is the damped exponential law. Considering that the incident photons are mono-energetic and mono-directional, we have

$$N^{(0)}(x,\mu,E) = \delta(E-E_0)\delta(1-\mu)\exp(-\Sigma(E_0)x)/2\pi, \quad (8)$$

where $\Sigma(E_0)$ is the mass attenuation coefficient of the photons with the initial energy E_0.

2.3. Single scattered photons' differential fluence

The uncollided photons suffer one time of Compton scattering at the place x, the scattered photons by electrons being called single scattered photons. The transport process of these single scattered photons is described by Eq.(6). The second term of the right-hand side of Eq.(6) is the single scattered photon source. By simple calculations we have

$$N^{(1)}(x,\mu,E) = H(E,\mu,E_0)\begin{cases}\exp[-\Sigma(E_0)x] - \exp[-\Sigma(E)x/\mu] & \mu\geq 0,\\ \dfrac{[\exp[\Sigma(E_0)(d-x)] - \exp[-\Sigma(E)(d-x)/\mu]}{\exp[\Sigma(E_0)d]} & \mu<0,\end{cases} \quad (9)$$

$$H(E,\mu,E_0)=\frac{K(E_0,E)\delta\left(\dfrac{mc^2}{E}-\dfrac{mc^2}{E_0}+\mu-1\right)}{2\pi[\Sigma(E)-\mu\Sigma(E_0)]}. \tag{10}$$

2.4. Multiple scattered photons' differential fluence

Multiple scattered photons result from two cases: one case is that through Compton scattering, single scattered photons become secondary scattered ones, which are brought into multiple scattered photons; another is that through Compton scattering multiple scattered photons which undergo Compton scattering again, still belong to multiple scattered photons. So the third and second terms on the right-hand side in Eq.(7) refer to the above-mentioned two kinds of multiple scattered photon source, respectively. To solve Eq.(7) we need to define the boundary and the initial conditions. The initial condition is

$$N^{(m)}(x,\mu,E_0)=0. \tag{11}$$

The boundary conditions are

$$N^{(m)}(0,\mu,E)=0 \quad \mu>0, \tag{12}$$

$$N^{(m)}(d,\mu,E)=0 \quad \mu<0. \tag{13}$$

Eq. (7) is, in fact, an ordinary differential equation, although it is in form an integral-differential equation. This is because, when we are to calculate the differential fluence of photons with energy E at various depths, we have already obtained the differential fluence of photons with energy higher than E at various points in space. This means that the source terms are already known. In order to make it clear, we use $S^{(1)}(x,\mu,E)$ and $S^{(m)}(x,\mu,E)$ to represent the contribution of single scattered photons to multiple scattered photon sources and the contribution of multiple scattered photons to multiple scattered photon sources, respectively, i.e.,

$$S^{(1)}(x,\mu,E)=\int_{4\pi}\mathrm{d}\boldsymbol{u}'\int_{E}^{E_0}\mathrm{d}E'N^{(1)}(x,\mu',E')K(E',E;\boldsymbol{u}\cdot\boldsymbol{u}'), \tag{14}$$

$$S^{(m)}(x,\mu,E)=\int_{4\pi}\mathrm{d}\boldsymbol{u}'\int_{E}^{E_0}\mathrm{d}E'N^{(m)}(x,\mu',E')K(E',E;\boldsymbol{u}\cdot\boldsymbol{u}'). \tag{15}$$

Now we start to solve Eq.(7) using the characteristic line method. Assume that $n+1$ directions are chosen, each directional cosine is a root of a Legendre polynomials of $(n+1)$ order, which satisfies

$$P_{n+1}(\mu_i)=0, \quad i=1,\cdots,n+1. \tag{16}$$

So the discretized Eq.(9) for photon transport is rewritten as

$$\mu_i\frac{\partial N^{(m)}(x,\mu_i,E)}{\partial x}=\Sigma(E)N^{(m)}(x,\mu_i,E)+S^{(1)}(x,\mu_i,E)+S^{(m)}(x,\mu_i,E). \tag{17}$$

Eq. (17) can be directly integrated. Taking the boundary conditions (12) and (13) into account, we have

$$N^{(m)}(x,\mu_i,E)=\begin{cases}\displaystyle\int_0^x\frac{\mathrm{d}x'}{\mu_i}[S^{(1)}(x',\mu_i,E)+S^{(m)}(x',\mu_i,E)]\exp\left[\frac{-\Sigma(E)(x-x')}{\mu_i}\right] & \mu_i>0;\\ \displaystyle\int_x^d\frac{\mathrm{d}x'}{|\mu_i|}[S^{(1)}(x',\mu_i,E)+S^{(m)}(x',\mu_i,E)]\exp\left[\frac{-\Sigma(E)|x-x'|}{|\mu_i|}\right] & \mu_i<0.\end{cases} \tag{18}$$

$S^{(1)}(x,\mu_i,E_k)$ and $S^{(m)}(x,\mu_i,E_k)$ can be figured out through $N_l^{(1)}(x,E')$ and $N_l^{(m)}(x,E')$. And then $N^{(m)}(x,\mu_i,E_k)$ and $N_l^{(m)}(x,E_k)$ can be found out. So we can further calculate the differential fluence and its harmonic moment of photons with energy E_k corresponding to the next energy point E_{k+1}. Repeating the above calculation procedure, we can obtain photon differential fluence at all energy points and all various depths.

3. The transport behaviour of secondary electrons produced by interactions between photons and atoms

3.1. Secondary electron sources produced by photon interactions

There occur three kinds of secondary electron sources due to photon interactions: photoelectron source $Q_{\rm photo}(x,\mu,E)$, Compton recoil electron source $Q_{\rm c}(x,\mu,E)$ and positron–electron pair source $Q_{\rm pair}(x,\mu,E)$. Assuming that the total secondary electron source is $Q(x,\mu,E)$, we have

$$\begin{aligned} Q(x,\mu,E) =& Q_{\rm photo}(x,\mu,E)+Q_{\rm c}(x,\mu,E) \\ &+Q_{\rm pair}(x,\mu,E). \end{aligned} \tag{19}$$

For photoelectron source, we have

$$\begin{aligned} &Q_{\rm photo}(x,\mu,E) \\ \approx&\frac{N_A}{A}\sigma_{\rm photo}(E)N(x,\mu,E), \quad E_k \ll E; \end{aligned} \tag{20}$$

$$\begin{aligned} &\sigma_{\rm photo}(E,E';\boldsymbol{u}\cdot\boldsymbol{u}') \\ \approx&\sigma_{\rm photo}(E)\delta(E'-E+E_k)\delta(1-\boldsymbol{u}\cdot\boldsymbol{u}')/2\pi, \end{aligned} \tag{21}$$

where E_k is the binding energy of k-shell electrons, $\sigma_{\rm photo}$ is the total cross section of photoelectrons. For Compton recoil electron source, we have

$$Q_{\rm c}(x,\mu,E)=\sum_{l=0}^{\infty}\frac{(2l+1)}{4\pi}P_l(\mu)Q_l^{\rm c}(x,E), \tag{22}$$

where $Q_l^{\rm c}(x,E)$ is equal to

$$\begin{aligned} Q_l^{\rm c}(x,E)=& \int_{\frac{E+\sqrt{E^2+2Em_0c^2}}{2}}^{E_0} {\rm d}E'\frac{N_AZ}{A}\frac{{\rm d}\sigma_{\rm c}}{{\rm d}E} \\ &\times P_l\left(\frac{1+\dfrac{m_0c^2}{E'}}{\sqrt{1+\dfrac{2m_0c^2}{E}}}\right)N_l(x,E'). \end{aligned} \tag{23}$$

Finally, for positron–electron pair source we have

$$\begin{aligned} \frac{{\rm d}^2\sigma_{\rm pair}}{{\rm d}T{\rm d}\Omega} =&\frac{{\rm d}\sigma_{\rm pair}}{{\rm d}T}\delta(\theta-<\theta>)/2\pi \\ \approx&\frac{{\rm d}\sigma_{\rm pair}}{{\rm d}T}\delta(1-\mu)/2\pi. \end{aligned} \tag{24}$$

Thus,

$$\begin{aligned} &Q_{\rm pair}(x,\mu,E) \\ =&\sum_{l=0}^{\infty}\frac{(2l+1)}{4\pi}P_l(\mu) \\ &\times\int_{E+2m_0c^2}^{E_0}\frac{N_A}{A}\sigma_{\rm pair}(E',E)N_l(x,E'){\rm d}E', \end{aligned} \tag{25}$$

and

$$\begin{aligned} &Q_{\rm pair}^{+}(x,\mu,E) \\ =&\sum_{l=0}^{\infty}\frac{(2l+1)}{4\pi}P_l(\mu)\int_{E+2m_0c^2}^{E_0}\frac{N_A}{A}\sigma_{\rm pair}(E',E'-E \\ &+2m_0c^2)N_l(x,E'){\rm d}E'. \end{aligned} \tag{26}$$

3.2. The transport and energy deposition of secondary electrons

Assuming that the differential fluence of secondary electrons is $N^{\rm e}(x,\mu,E)$, then using P_n approximation, we have

$$N^{\rm e}(x,\mu,E)=\sum_{l=0}^{n}\frac{(2l+1)}{4\pi}P_l(\mu)N_l^{\rm e}(x,E). \tag{27}$$

The spherical harmonic moment $N_l^{\rm e}(x,E)$ satisfies the following equation

$$\begin{aligned} &\frac{\partial N_l^{\rm e}\rho(E)}{\partial E}+\frac{1}{2l+1}\left[(l+1)\frac{\partial N_{l+1}^{\rm e}}{\partial x}+l\frac{\partial N_{l-1}^{\rm e}}{\partial x}\right] \\ =&-\varphi_l(E)N_l^{\rm e}+Q_l. \end{aligned} \tag{28}$$

The initial and boundary conditions are as follows:

$$N_l^{\rm e}(x,E_0)=0, \quad l=0,1,\cdots,n; \tag{29}$$

$$N^{\rm e}(0,\mu_i,E)=0, \quad i=0,1,\cdots,n, \quad \mu_i>0; \tag{30}$$

$$N^{\rm e}(d,\mu_i,E)=0, \quad i=0,1,\cdots,n, \quad \mu_i<0. \tag{31}$$

By using Lax–Wendroff scheme to solve Eqs.(28)–(31), we finally obtain the spectra of electrons at various depths $N_0^{\rm e}(x,E)$ and their spherical harmonic moments of each order.

4. Calculation results

In this section we give some typical results obtained by using our new algorithm. These results not only involve a comparison between the earlier results and our calculated results, but also consider the practical goal for developing this new algorithm, namely, applying it to clinical radiotherapy.

4.1. Calculation results of photon energy-fluence

For photon transport, the photon energy-fluence is a more important and more often used transport

quantity than photon fluence. By definition, photon energy-fluence is

$$I(x) = \int_0^{E_0} N_0(x, E) E \mathrm{d}E. \tag{32}$$

Having calculated the photon energy spectra $N_0(x, E)$ by using the theory presented in this paper, photon energy-fluence $I(x)$ can be worked out. Figure 1 illustrates the energy-fluence distributions of 1.0MeV photons in Be, H_2O, Cu and Pb. Figure 2 shows the energy-fluence distributions of 10.0MeV photons in Be, H_2O, Al, Cu and Pb. For comparison, we have used MCNP Monte Carlo code to calculate the energy-fluence distributions of photons with the same energies in the same media as above. It can be seen that the results calculated by using the characteristic line method are in good agreement with those calculated by using the MCNP Monte Carlo method. Therefore, the new method can meet the need of medical applications in accuracy.

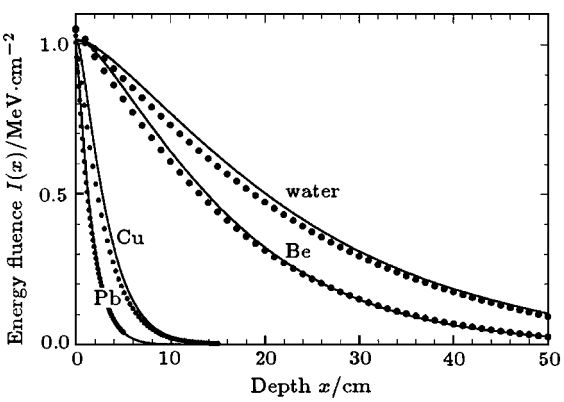


Fig.1. Energy fluence for 1.0MeV photon in difference media. Dots are the results calculated by MCNP, lines are our calculation results.

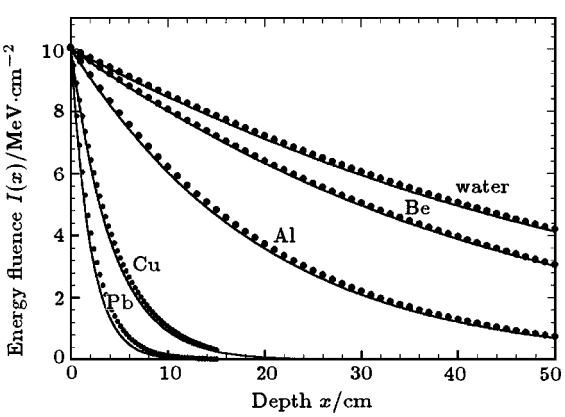


Fig.2. Energy fluence for 10MeV photon in difference media. Dots are the results calculated by MCNP, lines are our calculation results.

4.2. The energy deposition of photons in slab media

In so far as radiotherapy, the energy deposition distribution of high-energy photons in water or human body is a transport quantity which is followed with most interest. By definition, the energy deposition of photons at a certain point (i.e. absorbed dose) is

$$D(x) = \int_0^{E_0} N_0^{\mathrm{e}}(x, E) \left(\frac{\mathrm{d}E}{\mathrm{d}x}\right)_{\mathrm{T}} \mathrm{d}E, \tag{33}$$

where $(\mathrm{d}E/\mathrm{d}x)_{\mathrm{T}}$ is the total stopping power. Figure 3 shows the energy deposition distribution of photons with 1, 2, 3MeV energies in water. Figure 4 shows the energy deposition distribution of photons with 10MeV in water, Be, Al. From Figs.3 and 4 it can be seen that the absorbed dose distributions given by the characteristic line method are in good agreement with that given by the MCNP Monte Carlo method.

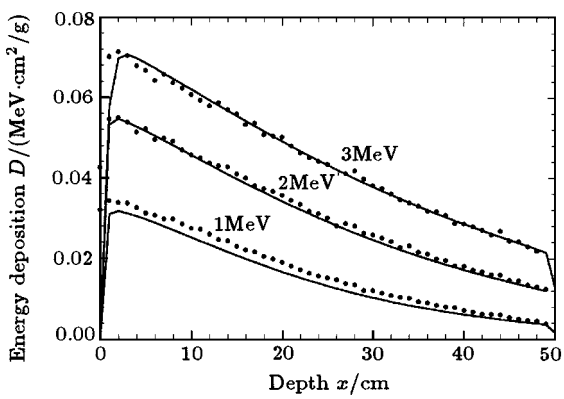


Fig.3. Energy deposition of photons with 1, 2, 3MeV energies in water. Dots are the results calculated by MCNP, lines are our calculation results.

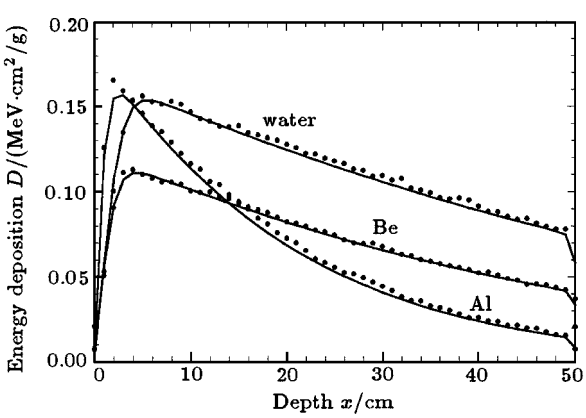


Fig.4. Energy deposition distribution of 10MeV photon in water, Be and Al Dots are the results calculated by MCNP, lines are our calculation results.

4.3. The efficiency of calculation

Compared with MNCP Monte Carlo method, an important advantage of our new theory and algorithms is its high calculation efficiency. This fact provides a good prospect for applying the method to clinical practice in radiotherapy. For this purpose we have made a systematical comparison. In order to make a reasonable comparison, we take the incident photon number to be 100,000 for Monte Carlo method, while taking the depth mesh to be 50, energy grid to be 50 and characteristic direction number to be 12 for the characteristic method. Calculations were conducted on the same PC machine with a 133MHz CPU. The computed results are listed in Table 1.

Table 1. A comparison of calculation time between the characteristic method and the MCNP method.

Method	Energy E/MeV	Calculation time t/s
MCNP4A	1	11817
	2	23452
	3	29901
	5	77399
	10	105753
Characteristic method	1	15
Only photon transport	2	15
	3	15
	5	15
	10	15
Characteristic method	1	16
(photon transport and	2	16
secondary electron transport)	3	16
	5	16
	10	16

As can be seen from Table 1, for photons with different energies (1MeV–10MeV), the characteristic method is $10^3 - 10^4$ times faster than the MCNP method. Calculation results clearly indicate that the newly developed photon transport theory is a very efficient algorithm, which is hopeful to find clinical applications in radiation therapy.

References

[1] 1976 ICRU Report 24, Determination of Absorbed Dose in a Patient Irradiated by Beams of X or Gamma rays in Radiotherapy Procedures p46

[2] Chandrasekhar S 1950 *Radiactive Transfer* (Oxford)

[3] Hopf E 1934 *Mathematical Problems of Radiative Equilibrium* (Cambridge Tracts No.31)

[4] Wick G C 1943 *Z. Phys.* **9** 702

[5] Goldstein H and Wilkins J E Jr 1954 *Calculations of the penetration of gamma rays* (NYO-3075 Nuclear Development Associates Inc)

[6] Spencer L V and Simons G L 1973 *Nucl. Sci. Eng.* **50** 20

[7] Takeuchi K 1973 PALLAS-PL, SP-A code dimensional transport code (Ship Research Institute, Japan) p42

[8] Gopinath D V and Samthanam K 1971 *Nucl. Sci. Eng.* **43** 186

[9] Shimizu A and Aoki K 1972 *Application of Invariant Embdding to Reactor physics* (New York: Academic)

[10] Radiation Shielding Information Center (RSIC) Code Collection. CCC-200 /MCNP, MCNP-A general Monte Carlo code for neutron and photon transport. Contribution by Los Alamos National Laboratory

[11] Nelson W R, Hirayama H and Rogers D W O 1985 *EGS4 Code System* (Stanford, CA: SLAC-265, Stanford Linear Accelerator Center)

[12] Boyer A and Mok E 1985 *Med. Phys.* **12** 169

[13] Ahnesjo A 1989 *Med. Phys.* **16** 577

[14] Zhu Y and Boyer A 1990 *Phys. Med. Biol.* **35** 351

[15] Bortfeld T, Schlegel W and Rhein B 1993 *Med. Phys.* **20** 311

[16] Siantar C L H *et al* 1997 *Proc. XIIth Int. Conf. on the Use of Computers in Radiation Therapy, Salt1 Lake City, UT*, May 27–30 (1997) 27–30